Hadronic- and electromagnetic-cores of air-showers observed by hybrid experiments at high mountains

M.Tamada
Faculty of Science and Engineering, Kinki University, Higashi-Osaka, 577-8502 Japan

Characteristics of the high energy families (bundle of high energy e,γ) and hadrons in the air-showers detected in the hybrid experiment together with emulsion chamber and AS-array at Mt.Chacaltaya are studied in detail by comparing with those of CORSIKA simulations using interaction models of QGSJET and EPOS. Because the atmospheric families and hadron component has more direct information of the nuclear interaction, correlations between atmospheric families and burst (hadron component of air-showers) accompanied to air-showers are more sensitive to the mechanism of the the cosmic-ray interactions. The burst size dependence of the family energy is compared with those of simulations. It is found that the family energy accompanied by the air-showers with the larger busrt-size is systematically smaller than that expected in the simulated events. The experimental results can not be described simply by changing chemical composition of primary cosmic-rays and this indicates x-distribution of secondary particles in the cosmic-ray interactions becomes much steeper than that assumed in the simulation models.

1. Introduction

The main interests of the cosmic-ray study now shift to the highest energy region, $E_0 \geq 10^{19}$ eV, using huge experimental apparatus to search astrophysical sources and acceleration or emission mechanism of those extreme high energy cosmic-rays. However, after a half of the century of its discovery, the "knee" in the cosmic-ray spectrum, steepening of the energy spectrum in $10^{15} \sim 10^{16}$ eV, is still not well understood. Because of the low intensities, direct observations of primary cosmic-rays in this energy range are still not possible and then various types of air-shower experiments at high mountains and also at ground level have been carried out in oder to investigate the chemical composition of primary cosmic-rays in this energy region which gives important physical origin of cosmic-rays [1–7]. The experimental data in those indirect measurement are usually interpreted by comparing with Monte Carlo simulations assuming some models of cosmic-ray interactions. Many of experimental groups claim that the fraction of heavy primaries increases rapidly beyond the "knee" region, e.g., the fraction of protons is estimated, by the Tibet AS-γ group shows[8], as small as $\sim$ 10 % of all particles in $E_0 = 10^{15} - 10^{16}$ eV. The results, however, depends on their assumed interaction model. For example, the model EPOS recently proposed[9, 10] gives muon numbers much more than QGSJET model does. The events which can be interpreted due to heavy primary when we employ QGSJET model as nuclear interactions are interpreted due to proton primary when EPOS is used as an interaction model [11]. Thus the interpretations heavily rely on the Monte Carlo calculations. In fact, various experimental groups give various data on chemical composition in these energy region and the results are still very confusing. We should examine whether the overall experimental data can be well interpreted by the assumed model before drawing a conclusion.

The hybrid experiments operating simultaneously an air-shower array, a hadron calorimeter and an emulsion chamber have been carried out at Mt. Chacaltaya (5200m, Bolivia)[1, 2], Yang-bajing (4300m, China)[3, 8] and Tien-Shan (3340m, Kazakhstan)[4] for studying cosmic-ray nuclear interaction in the energy region around $10^{15} - 10^{17}$ eV. In the hybrid experiments, we can obtain air-shower size, N_e, from the air-shower array data, particle-density, n_b, which are closely connected to the hadron component in the air-shower, from hadron calorimeter (busrt detector) and energy and geometrical position of individual high energy electromagnetic particle by the emulsion chamber. Correlations between air-showers and accompanying families were studied so far in these three experiments by comparing experimental data and simulated data[12, 13]. In the present paper we show some results obtained by studying correlations between hadron component (data of hadron calorimeters) and families observed by emulsion chamber which is considered to be very sensitive to the mechanism of cosmic-ray interactions, using data of Chacaltaya hybrid experiment.

2. Short summary of the analysis on air-showers and accompanied families

The shower-size, N_e, dependence on the family energy and on the lateral spread of the showers in the air-shower-triggered families were studied in the three hybrid experiments at high mountains. In Ref.[13] we have shown that the average of family energy normalized by associating air-shower size, $\Sigma E_\gamma / N_e$, of the events with $N_e \geq 10^7$ observed by in these hybrid experiments agree more or less to those expected in case of heavy-dominant composition of primary particles, as is shown in Fig.1, though the difference in

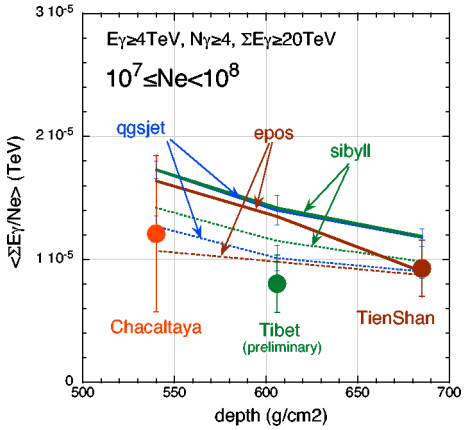

Figure 1: Depth dependence on the average family energy normalized by air-shower size for the events with $10^7 \leq N_e < 10^8$. Solid lines are for proton-dominant composition and dotted lines for heavy-dominant composition[13].

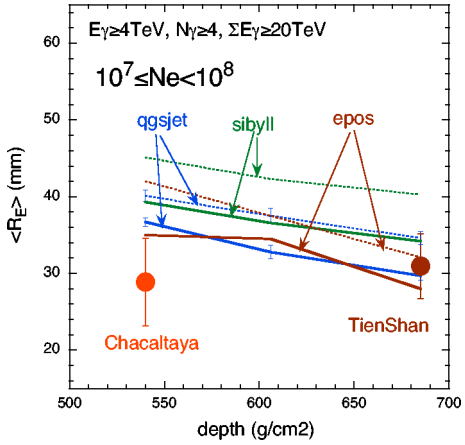

Figure 2: Depth dependence on the average lateral spread of EAS-triggered families with $10^7 \leq N_e < 10^8$[13].

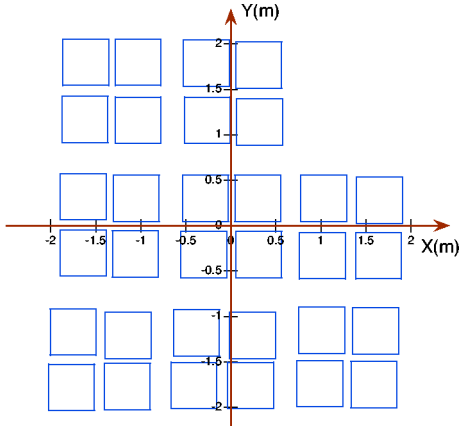

Figure 3: Configuration of 32 blocks of emulsion chambers and hadron calorimeters at the center of Chacaltaya air-shower array.

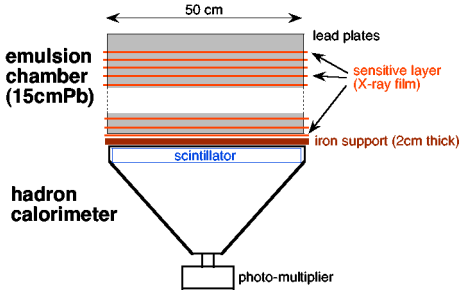

Figure 4: The structure (side view) of one of the block of the emulsion chamber and the hadron calorimeter (burst detector).

the average value between the two chemical composition, proton-dominant and heavy-dominant, is not clear in Tien-Shan altitude, specially in the case of EPOS model. Some detail of simulations are shown in Ref.[13]. The lateral spread of high energy showers in the families accompanied by the air-showers with $N_e \geq 10^7$ was also studied[1]. The average lateral spread of showers in those families observed by Chacaltaya experiment, shown in Fig.2, is found to be smaller than the one expected in case of heavy-dominant composition. The difference in the average lateral spread between the two chemical composition is again not clear in Tien-Shan data. The Chacaltaya data tell that the proton-dominant composition is favorable to explain small lateral spread of the families but the heavy-dominant composition is favorable to explain small family energy. Thus the increase of heavier composition of primary cosmic rays alone can not explain the general characteristics of air-shower-triggered families, contrary to the results of Tibet group and others.[5, 8, 14]

The data of hadron calorimeters were also analyzed by Chacaltaya and Tibet group. The Tibet group derived a conclusion from the analysis that the experimental data were well explained by heavy dominant composition of primary particles[3] but Chacaltaya group concluded that the number of hadrons in the air-showers was less than expected one[2].

[1]There is no official publication about the lateral spread of families accompanied by air-showers in Tibet $AS\gamma$ experiments.

3. Hybrid experiment at Mt.Chacaltaya

The air-shower array covers a circular area within a radius about 50 m by 35 plastic scintillation detectors to measure the lateral distribution of electron density of the air-showers. In the center of the air-shower array, 32 blocks of emulsion chambers (0.25 m^2 each) are installed (see Fig.3). Each block of the emulsion chamber consists of 30 lead plates of 0.5 cm thick each and 14 sensitive layers of X-ray film which are inserted at every 1 cm lead. The total area of the emulsion chambers is 8 m^2. Hadron calorimeters with plastic scintillator of 5cm thick are installed underneath the respective blocks of the emulsion chamber (see Fig.4). Iron support of 2 cm thick is inserted between the emulsion chamber and the hadron calorimeter. Some detail of the Chacaltaya hybrid experiment are described in Refs.[1, 2]

4. Simulations

4.1. Air-showers and families

For generating extensive air-showers and families we use CORSIKA simulation code(version 6.735) [15] employing QGSJET model (QGSJET01c)[16] and EPOS model (EPOS 1.60) [9, 10] for the cosmic-ray nuclear interaction. Primary particles of $E_0 \geq 10^{15}$ eV are sampled respectively from the power low energy spectrum of integral power index -1.7, for pure protons and pure irons, and also from the energy spectrum of primary cosmic rays with proton dominant and heavy dominant chemical composition. Some detail of chemical composition are shown in Table 1. The thinning energy is fixed to be 1 GeV. Shower size, N_e, at the observation point is calculated by using NKG option in the simulation. Air-shower center is randomly sampled within a area of ± 2.5 m in X and Y direction from the center of hadron detectors (see Fig.3).

4.2. High energy showers in emulsion chambers

For high energy (e,γ)-particles and hadrons of $E \geq$ 1 TeV, arriving upon each of the emulsion chamber, in the atmospheric families, we calculate further nuclear and electromagnetic cascade development inside the chamber taking into account exactly the structure of the emulsion chamber. We use QGSJET model for hadron-Pb interactions and a code formulated by Okamoto and Shibata for electromagnetic cascade[19]. The electron number density under every 1 cmPb is transformed into spot darkness of the X-ray film. Then the energy of each shower is re-estimated from the shower transition on spot darkness by applying the procedure used in the experiments.

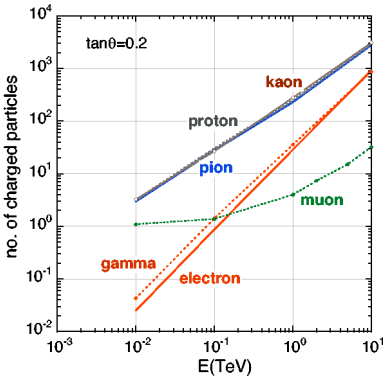

Figure 5: Energy dependence of average number of charged particles arriving to the scintillator of hadron calorimeter for π^-, proton, K^-, μ^-, e^- and γ incidence.

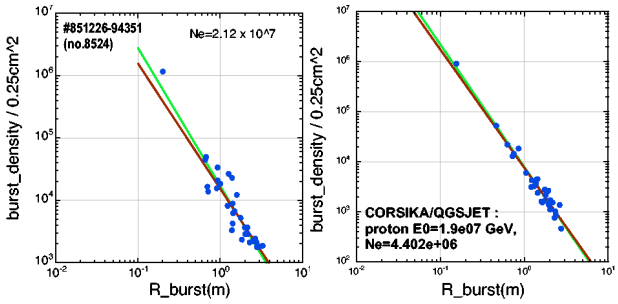

Figure 6: Examples of burst data in form of lateral distribution of burst-density for experimental data (left) and for simulated data of proton-primary (right).

4.3. Data of hadron calorimeters : Calculation of the burst-size

Hadron calorimeters detect a bundle of charged particles, which are produced in the emulsion chamber material by the hadron component in the air-shower through the local nuclear interactions. Output from each unit of the hadron calorimeter is related to the energy deposited in the scintillator, and it is converted to a charged particle number using average energy loss of a single muon in the scintillator. The number of charged particles per 50 cm $\times$ 50 cm, n_b, is called "burst density" hereafter. We use GEANT4 code[20] for calculating the burst-density. We calculate the average number of charged particles[2] produced in the emulsion chamber of 15 cmPb and arriving at the scintillator of hadron calorimeter for the hadrons (pions, proton, kaons), muons and high energy e, γ in the air-shower, with 4 different energies of 10 GeV, 100 GeV,

[2]Here we take into accounts a scintillator response of charged particles. Gamma-rays gives some energy deposit in the scintillator. Then the scintillator response of gamma-rays are also taken into accounts.[21]

Table I Chemical composition of primary cosmic-rays and air-showers

	sampled primary particles									
	proton dominant					heavy dominant				
E_0 (eV)	protons	He	CNO	heavy	Fe	protons	He	CNO	heavy	Fe
$10^{15} - 10^{16}$	42 %	16 %	16 %	14 %	12 %	17 %	10 %	18 %	15 %	40 %
$10^{16} - 10^{17}$	42 %	12 %	13 %	15 %	18 %	14 %	8 %	17 %	14 %	47 %
air-showers accompanied by burst (CORSIKA/QGSJET)										
	protons	He	CNO	heavy	Fe	protons	He	CNO	heavy	Fe
$10^6 < Ne < 10^7$	57 %	18 %	11 %	9 %	5 %	31 %	13 %	11 %	13 %	26 %
$10^7 < Ne < 10^8$	46 %	11 %	13 %	11 %	18 %	16 %	12 %	21 %	9 %	42 %
air-showers accompanied by families of $\Sigma E_\gamma \geq 10$ TeV (CORSIKA/QGSJET)										
	protons	He	CNO	heavy	Fe	protons	He	CNO	heavy	Fe
$10^6 < Ne < 10^7$	70 %	19 %	6 %	4 %	2 %	48 %	17 %	17 %	8 %	10 %
$10^7 < Ne < 10^8$	50 %	9 %	14 %	7 %	20 %	23 %	10 %	19 %	3 %	45 %

1 TeV and 10 TeV and 5 different zenith tangent of arrival direction. Fig.5 shows an example of the energy dependence of average number of charged particles which responds to scintillator for six different incident particles. The dependences are approximated by numerical functions and extrapolate to higher or lower energy range of the incident particles. Applying these functions to every particle incident upon the emulsion chamber, we get the burst-density in each block of 32 hadron calorimeters. We define n_b^{max} as the largest burst-density among 32 blocks of hadron calorimeters and Σn_b as the sum of burst-density of 32 blocks. In the following we pick up the events which satisfy the following criteria;

- $N_e \geq 10^6$,
- $n_b^{max} \geq 10^4$,
- $R_{AS-Bs} \leq 1$m,
  where R_{AS-Bs} is a distance between burst center and air-shower center.

The burst center is determined by the algorithm described in Ref.[2]. In the Chacaltaya data, 1,034 events satisfy the above criteria in ~ 40 m^{2}year exposure of hadron calorimeters. Among them 73 events are accompanied by high energy atmospheric families of $\Sigma E_\gamma \geq 10$ TeV ($E_{min} = 2$ TeV). Fig.6 show examples of experimental and simulated burst data. We can see the lateral distribution of the burst-density is well described by the power law function[2].

In Table 1, we show the fraction of proton, He, CNO, heavy and Fe components in the air-showers accompanied by families and also those accompanied by burst. In the shower-size region of $N_e \geq 10^7$, corresponding to $E_0 \approx 10^{16} - 10^{17}$ eV, the fraction of each component is similar to those assumed in the primary particles because almost all air-showers in this air-shower size region accompany families and bursts.

5. Correlation between air-showers and bursts

Fig.7 shows a scatter diagram between air-shower size, N_e, and maximum burst density, n_b^{max}, of the event for the experimental data and for the simulated data of proton- and Fe-primaries. In the events of iron-primaries, n_b^{max} is more or less proportional to N_e though n_b^{max} is weakly correlated to N_e for the events of proton primaries. It is very natural because Fe-air-nucleus interactions are assumed to be superposition of a number of low energy nucleon-air-nucleus collisions and then the fluctuation becomes small. But for proton-air-nucleus interactions, the position of interactions and/or released energy at the interaction fluctuate widely event by event. The distribution in the experimental data looks close to that in proton-primaries. Fig.8 show distributions of n_b^{max}/Ne for four different chemical composition of primary particles, pure proton, pure iron, proton-dominant and heavy dominant. The shape of the distribution for pure-iron primaries is very different from that for the others. There is almost no event with $n_b^{max}/Ne \geq\sim 0.02$ ($\log(n_b^{max}/Ne) \geq\sim -1.6$) in the iron-induced air-showers. On the contrary, considerable number of events are found in this region of the distribution in the proton-induced air-showers. There is no systematic difference in shape for the other three chemical compositions, pure protons, proton-dominant and heavy dominant[3] , and also for the two different interaction models, QGSJET and EPOS. The experimental data are well described by the model calculation

[3]Nearly a half of the air-showers accompanied by bursts are due to protons and He-nuclei, even when heavy-dominant chemical composition is assumed in primary particles, as is seen in Table 1. This is a reason why the difference in the shape of the distribution among these three chemical compostion is small.

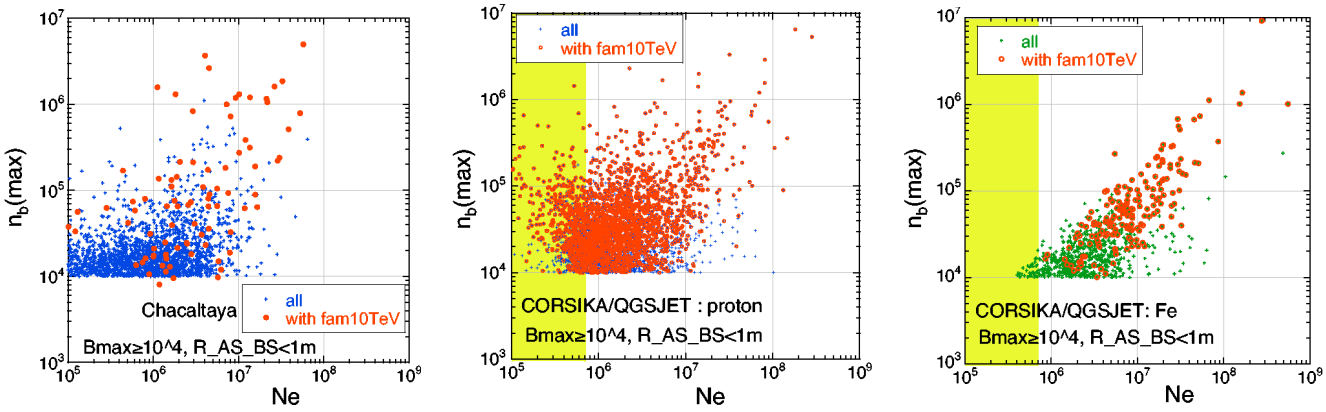

Figure 7: Scatter diagram between air-shower size, N_e, and maximum burst density, n_b^{max}, of the event. Shaded area in the simulated data is biased because the sampled primary energy is larger than 10^{15} eV.

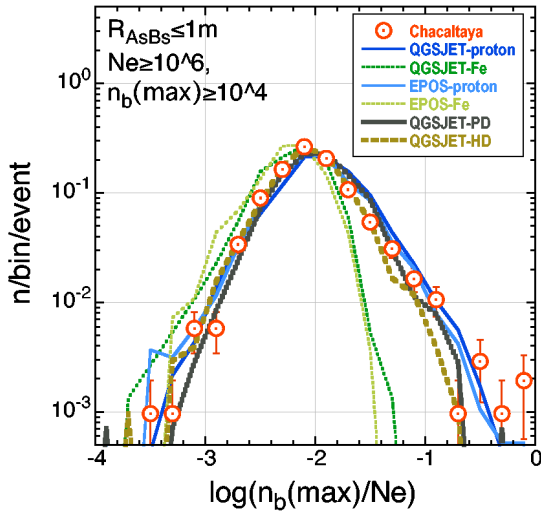

Figure 8: Distribution of n_b^{max}/Ne. Circles are experimental data and lines are simulated data, solid lines : proton-primaries, dotted lines : Fe-primaries.

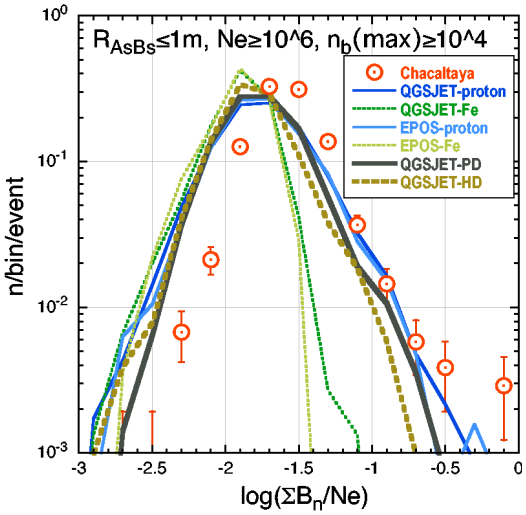

Figure 9: Distribution of $\Sigma n_b/Ne$. Circles are experimental data and lines are simulated data, solid lines : proton-primaries, dotted lines : Fe-primaries.

for these three chemical compositions of primary particles. Fig.9 shows that of $\Sigma n_b/Ne$ where Σn_b is a sum of n_b over 32 blocks of hadron calorimeters. Again we can see the experimental data are close to those expected in pure protons or mixed chemical composition of proton-dominant and heavy-dominant, though the number of events with smaller Σn_b are less than expectation. The almost same analysis was done by Tibet group and they concluded that their data are well described by heavy dominant composition (see Ref.[3]).

6. Correlation between bursts and families

Fig.10 shows a correlation diagram between n_b^{max}, maximum of burst size among 32 blocks of the event and accompanying family energy. The experimental data are compared with those of simulated data of proton-primaries and iron-primaries. As is seen in the figure, the family energy is almost proportional to n_b^{max} in the simulated data irrespective of the primary particles though the family energy of the events coming from iron-primaries are smaller than that from proton-primaries. In the figure we can see the family energy in the experimental data is systematically smaller than that of simulated data in the events with larger burst-density, $n_b^{max} \geq 10^5$. Fig.11 shows an average family energy versus n_b^{max}. It is clear that

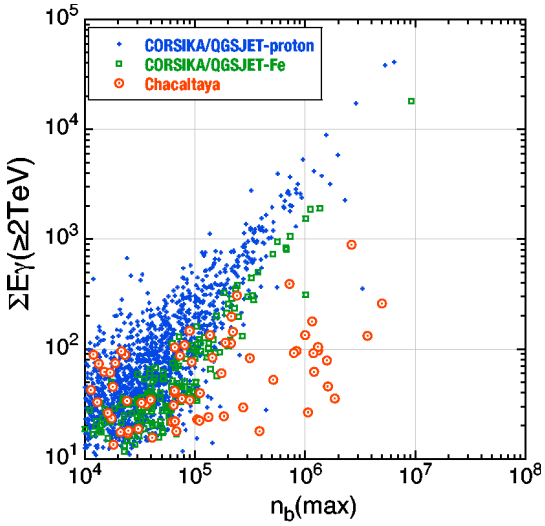

Figure 10: Correlation diagram between n_b^{max} and family energy ΣE_γ in the burst-triggered families in the air-showers of $N_e \geq 10^6$.

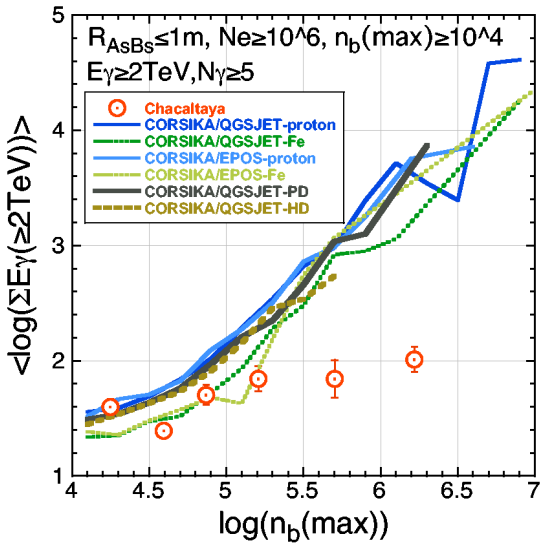

Figure 11: Average family energy versus n_b^{max} in the burst-triggered families.

the experimental data can not be explained simply by changing chemical composition of primary particles.

One may argue that the smaller family energy in the experimental data is due to the systematic underestimation of the shower energy in the emulsion chamber. Fig.12 shows a comparison of the integral spectra of family energy observed by the present hybrid experiment and that by the emulsion chamber experiment of Brazil-Japan collaboration[22]. As is seen in the figure, the two spectrum smoothly connected each other. Thus we can conclude the energy estimation of high energy particles in the emulsion chamber of the present hybrid experiment is not much different from that of emulsion chamber experiment of Brazil-Japan collaboration.

One may also argue about overestimation of the burst-density, specially beyond the region of $n_b \geq 10^5$. But this possibility is also ruled out, because the distribution on n_b^{max}/N_e is well described by the simulations as is seen in Fig.8.

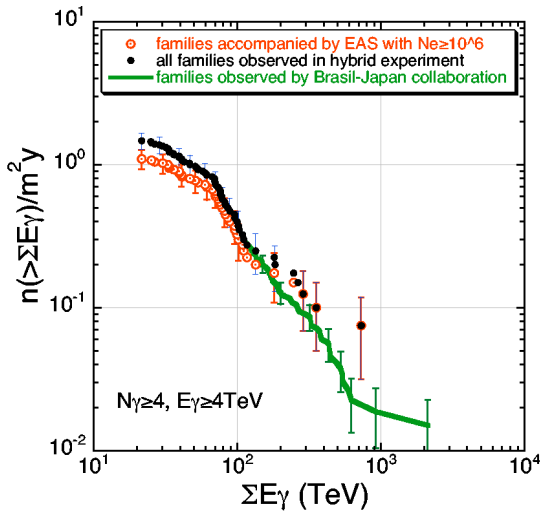

Figure 12: Comparison of the integral family energy. Solid line is for the emulsion chamber experiment of Brazil-Japan Collaboration and solid circles are for air-shower triggered families and open circles are for all families observed in the present hybrid experiment.

7. Discussions

The previous analysis on the air-shower-triggered families shows that the average familiy energy of the experimental data is considerably smaller than that of simulations of proton-dominant primaries in the shower size region of $Ne \geq 10^7$, as described in section 2. In Fig.13 we show a correlation diagram between family energy, ΣE_γ and associated air-shower size, N_e for the same events shown in Fig.10. In the air-shower-size region of $N_e \geq 10^7$, the family energy in the experimental data is systematically smaller than that expected in case of proton-primaries and those events look like coming from iron-primaries.

The characteristics of the bursts accompanied by the proton-induced air-showers are very different from those accompanied by iron-induced ones, as is shown in Fig.7. The considerable number of air-showers induced by proton-primaries accompany large burst-density which are not seen in the iron-induced air-showers, and the experimental data are close to those expected in case of proton-primaries. The contradiction of the above two arguments is well seen in the

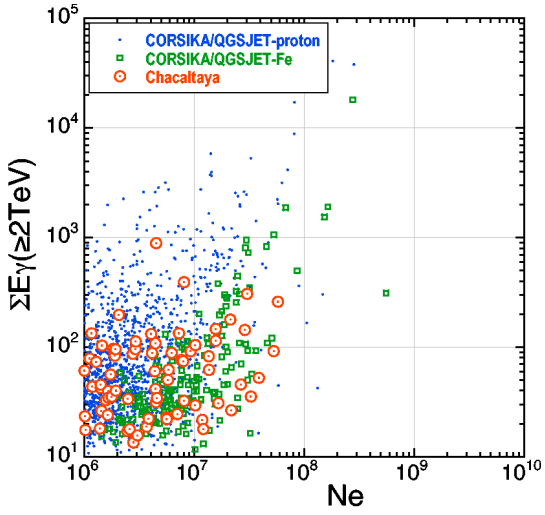

Figure 13: Correlation diagram between air-shower size, N_e, and accompanied family energy, ΣE_γ, of the events shown in Fig.10.

correlation digram between bursts and families, shown in Fig.10 and no model can describe the observed correlation.

The spectra of high energy particles detected by the emulsion chambers are more sensitive to the mechanism of the particle production of the most forward region of the rapidity. The hadron calorimeter supplies the data of hadron component in the air-shower. The hadron component in the air-shower bears more direct information on the nuclear interaction than any other component such as electron and muon component in the air-shower and the burst-size of hadron calorimeter gives a measure of interaction energy.

Suppose x-distribution of the produced particles becomes steeper, the number of high energy particles detected in the emulsion chamber becomes small (i.e., detected family energy becomes smaller), because of high threshold energy of the emulsion chambers. The hadron component detected by hadron calorimeters, however, does not much changed because of lower detection threshold energy. Then the ration of $\Sigma E_\gamma / n_b^{max}$ becomes smaller. The observed discrepancy between experimental data and simulated data can be explain in this way, that is, the experimental data indicate the x-distribution of produced particles in the cosmic-ray nuclear interactions of $E_0 \geq\sim 10^{16}$ eV is much steeper than that assumed in the models.

Acknowledgments

The author wishes to thank all the member of Chacaltaya hybrid experimemt, especially to Drs. N.Kawasumi, K.Honda, N.Ohmori, N.Inoue and A.Ohsawa for their valuable comments and discussions on the details of experimental procedures.

References

[1] N.Kawasumi et al., Phys. Rev. D **53** (1996) 3534
[2] C.Aguirre et al., Phys. Rev. D **62** (2000) 032003
[3] Tibet ASγ Collaboration (M.Amenomori et al.), Phys. Rev. D **62** (2000) 112002-1, 072007-3
[4] S.B.Shaulov, AIP Conf. Proc. **276** (1992) 94
[5] Y.Shirasaki et al., Astropart. Phys. **15** (2001) 357
[6] T.Antoni et al. KASCADE Collboration, Astropart. Phys. **14** (2001) 245, **19** (2003) 703,715
[7] S.P.Swordy et al., Astrop. Phys. **18** (2002) 129
[8] Tibet ASγ Collaboration (M.Amenomori et al.), Phys. Lett. B **632** (2006) 58
[9] K.Werner, F.M.Liu and T.Pierog, Phys. Rev. C **74** (2006) 044902
[10] T.Pierog and K.Werner, Proceedings of 30th ICRC, Merida (2007), Vol.4, p.629
[11] H.Urlich et al., Proceedings of 30th ICRC, Merida (2007), Vol.4, p.87
[12] H.Aoki et al., Proceedings of 30th ICRC, Merida (2007), Vol.4, p.23
[13] S.P.Besshapov et al., Nucl. Phys. B (Proc. Suppl.) 196(2009) 118; Proceedings of 31th ICRC, Lodz (2009) #0214
[14] J.R.Horandel, Astropart. Phys. **19** (2003) 193
[15] D.Heck, J.Knapp, J.N.Capdevielle, G.Schatz and T.Thouw, Fortshungzentrum Karlsruhe, FZKA 6019 (1998)
[16] N.N.Kalmykov and S.S.Ostapchenko, Yad. Fiz. **56** (1993) 105
[17] R.S.Fletcher et al., Phys. Rev. **D50** (1994) 5710
[18] J.Engel et al., Phys. Rev. **D46** (1992) 5013,
[19] M.Okamoto and T.Shibata, Nucl. Instr. and Meth. A **257** (1987) 155
[20] S.Agostinlli et al. Geant4 collaboration, Nucl. Inst. and Meth. A506(2003) 250
[21] N.Ohmori, private communication.
[22] C.M.G.Lattes, Y.Fujimoto and S.Hasegawa, Phys. Rep. Vol.65 (1980) 151